Journal of Electronic Research and Application, 2026, Volume 10, Issue 3
http://ojs.bbwpublisher.com/index.php/JERA
ISSN Online: 2208-3510
ISSN Print: 2208-3502

Shadow Thermodynamics of an AdS Black Hole in Non-Commutative Geometry

Ying Zhu*, Qing-Quan Jiang

School of Physics and Astronomy, China West Normal University, Nanchong 637002, China

**Author to whom correspondence should be addressed.*

Abstract: In this paper, we innovatively adopt the shadow radius to investigate the thermodynamics of an AdS black hole with non-commutative geometry terms. First, via geodesic analysis, we establish a quantitative relationship between the shadow radius and the event horizon radius, and derive the shadow radius of the black hole as a function of the event horizon radius, which exhibits a positive correlation between the two quantities. Furthermore, within the shadow framework, we find that the stability and heat capacity of the black hole can be effectively represented through the shadow radius. Further analysis reveals that the results obtained using the shadow radius in revealing the black hole phase transition process are essentially consistent with those obtained using the event horizon. Based on this, we constructed the thermal profile for an AdS black hole incorporating non-commutative parameters. Within the framework of non-commutative geometry, for $P < Pc$, the temperature derived from the shadow radius exhibits a distinct N-shaped trend, which is in perfect agreement with that obtained from the event horizon radius. This result reveals that even in non-commutative spacetime, the phase transition process of AdS black holes can be effectively and intuitively characterized by the thermal profiles of their shadows.

Keywords: Black hole; Shadow thermodynamics; Non-commutative geometry; Quantum gravity; Critical phenomenon

Online publication: April 24, 2026

1. Introduction

In Einstein's theory of general relativity, black holes are predicted as a type of celestial body in the universe [1]. Currently, astronomers and physicists have devoted extensive attention and conducted in-depth investigations into the theoretical and experimental studies of black hole physics. As a thermodynamic system, black holes possess properties such as temperature, entropy, and heat capacity. The study of black hole thermodynamics has significantly advanced the development of black hole physics. In recent decades, physicists have gathered extensive astronomical evidence regarding black holes, with the observation of gravitational waves pioneering new approaches to studying their properties. The detection of gravitational wave signals from the merger of two

black holes by the Laser Interferometer Gravitational-Wave Observatory (LIGO) provides compelling evidence for the existence of black holes [2]. In 2019, the Event Horizon Telescope (EHT) collaboration reported the ultra-high-resolution image of the supermassive black hole M87*, providing direct evidence that black holes truly exist in the universe and opening new frontiers for research in black hole observation [3–9]. This image reveals a dark central region surrounded by a bright ring, where the dark region is defined as the black hole shadow and the bright ring as the photon ring. Due to the intense gravitational field near a black hole, light undergoes deflection [10]. For a static observer at infinity, photons with an orbital radius smaller than the critical bound photon orbit radius fall into the black hole, thus forming the black hole shadow [11]. In contrast, other photons escape to infinity. This critical bound orbit is the black hole's photon ring. The size and shape of the black hole shadow are determined by this photon ring [12–17].

Studies of black hole shadows can yield more valuable geometric information about black holes, and observations of these shadows enable a deeper understanding of their intrinsic properties. For a Schwarzschild black hole, the photon ring is located at $r = 3M$ [18,19]. The study of photon trajectories in Schwarzschild black holes was pioneered by Synge and Luminet, and Bardeen subsequently investigated the shadow of the rotating Kerr black hole [10,20]. As more physicists conduct research on black hole shadows, it has been discovered that these shadows can be used to test Lorentz symmetry [21,22]. Furthermore, by considering the accretion around black holes, the study of shadows for diferent types of black holes has yielded significant results [12,14,23–38].

Based on this, investigating the unique thermodynamic properties of black holes as thermodynamic systems has become a key objective for many physicists. However, a deeper understanding of black hole thermodynamics began with the establishment of the four laws of black hole thermodynamics and was significantly deepened and substantiated by the discovery of Hawking radiation. Stephen Hawking, by applying quantum field theory, demonstrated that due to vacuum quantum fluctuations, particles can be emitted from the vicinity of a black hole's event horizon (known as Hawking radiation) [39]. This discovery laid a solid foundation for the theory of black hole thermodynamics. Based on the foundational assumptions of the "cosmic censorship hypothesis" and the validity of the "strong energy condition", Hawking proved the proposition known as "Hawking's area theorem" which states that the total area of a black hole's event horizon never decreases within the framework of classical physics. Secondly, the entropy and temperature of a black hole are expressed through the area of its event horizon and its surface gravity [40]. Based on this research, the fundamental framework of the four laws of black hole thermodynamics was established. Within Anti-de Sitter (AdS) spacetime, it has been discovered that the thermodynamic system of a charged AdS black hole is essentially equivalent to a van der Waals fluid-gas system [41–44]. Pioneering work by Wei *et al.* first explored the dynamic phase behavior of charged AdS black holes within the extended phase space framework and established the fundamental connection between black hole thermodynamics and the shadow radius [45]. Subsequently, Zhang *et al.* provided initial evidence that the shadow radius can indeed reflect the thermodynamic phase structure of black holes [46,47].

The black hole shadow serves as a bridge reflecting thermodynamic information of black holes, and combining the two for research holds significant importance. In summary, studies on black hole thermodynamics and their shadows remain very extensive in recent years. This paper primarily investigates the relationship between the black hole shadow radius and thermodynamic phase transitions in the AdS spacetime. Research demonstrates that the black hole shadow can indeed reveal the process of thermodynamic phase transitions. Furthermore, in the context of regular spacetime, it is found that the dependency relationship between the black hole shadow and thermodynamics is likely to be structurally established [29,48].

Furthermore, non-commutative spacetime in gravitational theory is a prominent research topic, as it is regarded as a potential candidate for quantum gravity [49,50]. Studying the influence of non-commutativity on black holes constitutes a highly significant research topic, and several methods can be employed to realize non-commutative spacetime within gravitational theory [51–55]. Secondly, it is demonstrated that within the framework of general relativity, non-commutativity can be implemented by modifying the source of matter, whereby a Gaussian distribution or a Lorentzian distribution can replace the Dirac delta function [56, 57]. Taking the AdS black hole with a non-commutative parameter as an example, this paper investigates the thermodynamic phase transitions under the shadow radius.

2. AdS black hole in non-commutative geometry

Non-commutative geometry is a theory of spacetime quantization, in which the commutation relations of spacetime coordinate operators can be expressed as [45]:

$$[x^{\mu}, x^{\nu}] = i\theta^{\mu\nu} \tag{1}$$

In non-commutative geometry, the Lorentz distribution ρ of the mass density for spherically symmetric stars is given by [57]:

$$\rho = \frac{M\sqrt{\theta}}{\pi^{3/2}(r^2+\pi\theta)^2} \tag{2}$$

Here, M denotes the black hole mass and θ the non-commutative parameter, which characterizes the minimal spacetime scale.

The Einstein equation is:

$$R_{\mu\nu} - \frac{1}{2}g_{\mu\nu}R + \Lambda g_{\mu\nu} = 8\pi T_{\mu\nu} \tag{3}$$

$R_{\mu\nu}$ is the Ricci tensor, which describes the curvature of spacetime; $g_{\mu\nu}$ is the metric tensor, which simplifies the expressions of the Einstein field equations and ensures their invariance under diferent coordinate systems; R is the Ricci scalar, which represents a global measure of spacetime curvature; $T_{\mu\nu}$ is the energy-momentum tensor, which describes the distribution of matter and energy in spacetime.

In non-commutative scenarios, a Schwarzschild black hole is:

$$ds^2 = -f(r)dt^2 + f^{-1}(r)dr^2 + r^2d\Omega^2 \tag{4}$$

Substituting **Equation (4)** into **Equation (3)** yields:

$$f(r) = 1 + \frac{1}{r}\int_0^r \left(8\pi r^2 T_0^0 - r^2\Lambda\right)dr \tag{5}$$

T_0^0 represents the energy density.

According to the Lorentz distribution formula in **Equation (2)**, we have:

$$T_0^0 = -\rho = -\frac{M\sqrt{\theta}}{\pi^{3/2}(r^2+\pi\theta)^2} \tag{6}$$

By substituting the above equation into the metric, we can obtain:

$$f(r) = 1 + \frac{1}{r}\int_0^r \left(-8\pi r^2 \frac{M\sqrt{\theta}}{\pi^{\frac{3}{2}}\left(r^2+\pi\theta\right)^2} - r^2\Lambda\right) \tag{7}$$

in which [58]:

$$f(r) = 1 - \frac{2M}{r} + \frac{8M\sqrt{\theta}}{\sqrt{\pi}r^2} - \frac{\Lambda}{3}r^2 + \mathcal{O}(\theta^{3/2}) \quad (8)$$

In the limit $\theta \to 0$, the spacetime geometry reduces to the standard Schwarzschild geometry. For the sake of simplicity, this article introduces a new parameter α.

$$\alpha = \frac{8\sqrt{\theta}}{\sqrt{\pi}} \quad (9)$$

The metric of Schwarzschild-AdS BH in non-commutative geometry:

$$f(r) = 1 - \frac{2M}{r} + \frac{\alpha M}{r^2} - \frac{\Lambda}{3}r^2 \quad (10)$$

The cosmological constant, Λ, is defined as $\Lambda = -8P\pi$. For a black hole to exist, the following conditions must be satisfied: $f(r_H) = 0$, $r_H > 0$, $M > 0$, $\Lambda < 0$, so there are the following inequalities that depend on α.

$$-2r^3{}_H + \alpha r^2{}_H < 0 \quad (11)$$

$$r^4{}_H - 2Mr^2{}_H - \alpha M r^2{}_H < 0 \quad (12)$$

Based on **Equation (4)**, in the context of static spacetime, The Lagrangian L can be expressed as:

$$\mathcal{L} = \frac{1}{2} g_{\mu\nu}\dot{x}^{\mu}\dot{x}^{\nu} = \frac{1}{2}(-f(r)\dot{t}^2 + f(r)^{-1}\dot{r}^2 + r^2(d\vartheta^2 + sin^2\vartheta d\varphi^2)) \quad (13)$$

In a spherically symmetric spacetime, we study photons moving on the equatorial plane with $\theta = \pi/2$. Furthermore, the metric functions do not depend on the time t and the azimuthal angle φ . Consequently, the equations associated with the constants of motion can be derived. These constants are:

$$E = -\frac{\partial \mathcal{L}}{\partial \dot{t}} = f(r)\dot{t}, L = \frac{\partial \mathcal{L}}{\partial \dot{\varphi}} = r^2\dot{\varphi} \quad (14)$$

The photon's energy and angular momentum are denoted by E and L, respectively. Consequently, for the given line element, the null geodesic condition $g_{\mu\nu}\, x^{\cdot\mu} x^{\cdot\nu} = 0$ can be expressed as:

$$-f(r)\dot{t}^2 + \frac{\dot{r}^2}{f(r)} + r^2\varphi^2 = 0 \quad (15)$$

Then, according to **Equation (14)** and **Equation (15)**, we can obtain:

$$\dot{r}^2 = E^2 - \frac{L^2}{r^2}f(r) \quad (16)$$

The radial geodesic motion can be described by the following equation for the effective potential V_{eff}.

$$r^2 + V_{eff} = 0 \quad (17)$$

The quantity b denotes the impact parameter, which is defined as the ratio L/E and geometrically corresponds to the perpendicular distance from the geodesic to a radial line through the origin. Finally, we can obtain the effective potential V_{eff} as:

$$V_{eff} = \frac{f(r)}{r^2}L^2 - E^2 \quad (18)$$

Where [59]:

$$E^2 = -\frac{f(r)}{r}\frac{df(r)}{dr}, L^2 = l(l+1) \quad (19)$$

In **Figure 1**, we analyze the non-commutative Lorentz effective potential, and investigate its functional dependence on r_H for different values of α. **Figure 1** shows the effect of the non-commutative parameter α on the effective potential for a massive test particle. When α is non-zero, all extrema of the non-commutative effective potential lie outside the non- commutative event horizon. Increasing α lowers the maximum peak of the effective

potential and shifts it further from the horizon. The divergence of the effective potential near the event horizon arises from non-commutative geometry, which acts as a potential barrier to prevent high-energy particles from falling into the black hole.

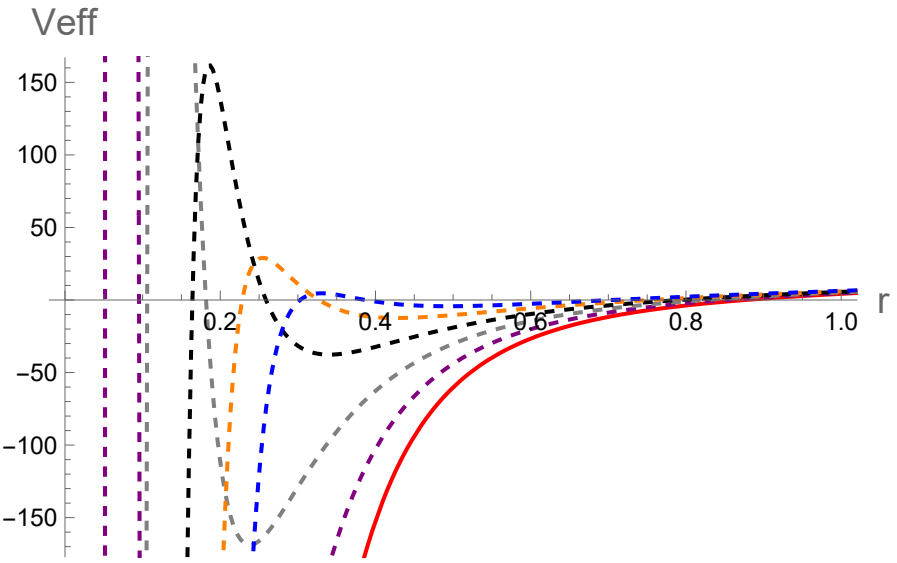

Figure 1. The effective potential α = 0, (Red solid line), α = 0.1, (Purple dashed line), α = 0.2, (Gray dashed line), α = 0.3 (Black Dashed line), α = 0.4 (Orange dashed line), α = 0.5 (Blue dashed line). P = 0.2, M = 1, L = 1.

3. Shadow radius of Schwarzschild-AdS black hole in non-commutative geometry

The following conditions must be satisfied for the effective potential to exist

$$V_{eff}(r) = 0,\ V'_{eff}(r) = 0,\ V''_{eff}(r) > 0 \tag{20}$$

Here, we denote the radius of the photon sphere as r_{pH}. For a given metric function, we can determine r_{pH} by solving the equation.

$$f(r_{pH}) - \frac{1}{2} r_{pH} f'(r_{pH}) = 0 \tag{21}$$

$$r_{pH} = \frac{1}{2}(3M + \sqrt{M}\sqrt{9M - 8\alpha}) \tag{22}$$

The black hole mass, which is also identified as enthalpy in the extended phase space, is given by the condition $f(r_H) = 0$.

$$M = \frac{r^2_H\,(3+8P\pi r^2_H)}{3(2r_H - \alpha)} \tag{23}$$

The shadow radius of a black hole is a crucial observable that provides insights into its fundamental properties. By analyzing the shadow, we can infer the black hole's mass, spin, and nature of spacetime surrounding it. Observing a black hole's shadow allows us to delve deeper into its physical characteristics and the role gravity plays in the universe. It represents the radius of the circular region projected by the black hole's event horizon as viewed by distant observers. The shadow radius, denoted by r_0, observed from a position at r_0 is given by the following equation [60].

$$r_s = r_{pH}\sqrt{\frac{f(r_0)}{f(r_{pH})}} \tag{24}$$

With the static observer at spatial infinity, we set the observer's radial coordinate to $r_0 = 100$, satisfying the condition $f(r_0) = 1$. Therefore, the shadow radius rs is:

$$r_s = r_{pH}\sqrt{\frac{1}{1+\frac{8}{3}P\pi r_{pH}^2+\frac{M(-2r_{pH}+\alpha)}{r_{pH}^2}}} \tag{25}$$

$$r_{pH} = \frac{1}{2}\left(\frac{r_H^2(3+8P\pi r_H^2)}{2r_H-\alpha}+\sqrt{\frac{r_H^2(3+8P\pi r_H^2)}{6r_H-3\alpha}}\sqrt{-8\alpha\frac{3r_H^2(3+8P\pi r_H^2)}{-2r_H+\alpha}}\right) \tag{26}$$

Figure 2 depicts the relationship between the black hole shadow radius rs and the event horizon radius rH for different values of the non-commutative parameter α. The results show that the shadow radius rs increases with the event horizon radius r_H, while the growth rate gradually decreases. This demonstrates a positive correlation between r_H and r_s, suggesting that the shadow radius can serve as an indicator of the black hole's Hawking temperature. Furthermore, the shadow radius r_s decreases with increasing pressure P. For a fixed horizon radius, increasing the non-commutative parameter α also leads to a decrease in r_s.

When the non-commutative parameter α approaches zero, the black hole model reduces to a Schwarzschild-AdS black hole. As shown in **Figure 2(a)**, the Schwarzschild-AdS black hole also exhibits a positive correlation α between r_H and r_s. Therefore, we conclude that the shadow radius can effectively describe the black hole temperature, similarly to the event horizon radius.

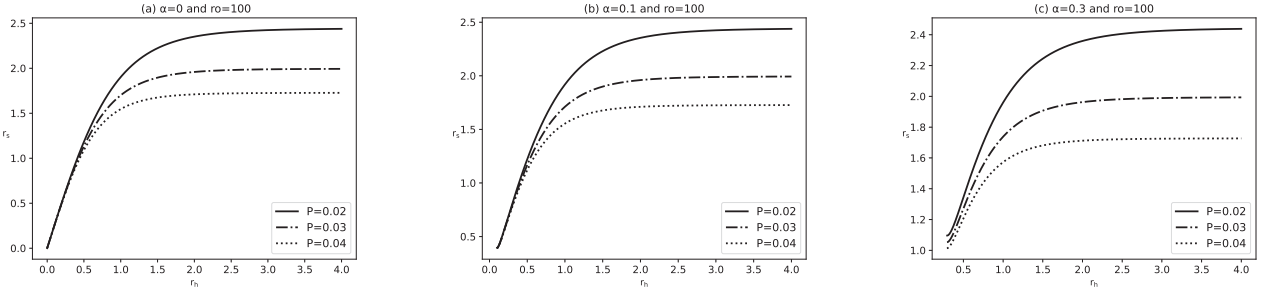

(a) (b) (c)

Figure 2. The relationship between shadow radius and the horizon radius. (a) Non-commutative parameter α = 0, r_0 = 100 (Schwarzschild-Ads BH), (b) Non-commutative parameter α = 0.1, r_0 = 100, (c) Non-commutative parameter α = 0.3, r_0 = 100. The solid lines, segment point lines and dotted lines correspond to P = 0.02, P = 0.03 and P = 0.04, respectively.

Next, let's calculate some fundamental thermodynamic quantities. The black hole's mass is

$$M = \frac{r_H^2(3+8P\pi r_H^2)}{3(2r_H-\alpha)} \tag{27}$$

A black hole's temperature is its Hawking temperature, determined by its surface gravity,

$$T = \frac{f'(r_H)}{4\pi} = \frac{3r_H-3\alpha-3r_H^3\Lambda+2r_H^2\alpha\Lambda}{12\pi r_H^2-6\pi r_H\alpha} \tag{28}$$

To study criticality, a specific volume, $v = 2r_H$, was introduced. Using this relationship, the equation of state becomes:

$$P = -\frac{3v-6\pi Tv^2-6\alpha+6\pi Tv\alpha}{6\pi v^3-8\pi v^2\alpha} \tag{29}$$

The black hole's entropy satisfies the Bekenstein-Hawking relation.

$$S = \frac{A}{4} = \pi r_H^2 \tag{30}$$

where $A = 4\pi r_H^2$ is the surface area of the black hole's event horizon.

However, when the energy-momentum tensor T_0^0 includes the black hole's mass, the traditional first law of thermodynamics, dM = TdS +VdP is violated, as shown by the following relations.

$$T \neq \left(\frac{\partial M}{\partial S}\right)_P, V \neq \left(\frac{\partial M}{\partial P}\right)_S \tag{31}$$

The modified first law of thermodynamics can be expressed as:

$$dM = WdM = TdS + V\,dP \tag{32}$$

Here, W represents the correction function.

$$W = 1 + \int_{r_H}^{+\infty} 4\pi r^2 \frac{\partial T_0^0}{\partial M} dr = 1 - \frac{\alpha}{2r_h} + O(\alpha^3) \tag{33}$$

Using the modified first law, we can derive the Hawking temperature.

$$T = W\left(\frac{\partial M}{\partial S}\right)_P = \frac{f'(r_H)}{4\pi} = \frac{3r_H - 3\alpha - 3r_H^3\Lambda + 2r_H^2\alpha\Lambda}{12\pi r_H^2 - 6\pi r_H \alpha} \tag{34}$$

The black hole's thermodynamic volume also can be derived.

$$V = W\left(\frac{\partial M}{\partial P}\right)_S = \frac{4\pi r_H^3}{3} \tag{35}$$

This result is consistent with those derived from the general thermodynamics of black holes. The critical point must meet:

$$\frac{\partial^2 P}{\partial (r_H)^2} = \frac{\partial P}{\partial (r_H)} \tag{36}$$

The critical condition is:

$$P_c = \frac{0.0027338}{\alpha^2}, T_c = \frac{0.036403}{\alpha}, r_c = 2.44155\alpha \tag{37}$$

4. Shadow analysis of non-commutative phase transitions in Schwarzschild-AdS black holes

In this section, we first investigate the thermodynamic phase transitions of non- commutative Schwarzschild-AdS black holes with a Lorentzian potential. Based on our previously derived Hawking temperature formula, the black hole temperature varies continuously with the event horizon radius r_H. As shown in **Figure 3(a)**, the black hole temperature exhibits distinct behaviors under different pressure conditions:

(1) When (P = 1.4Pc), the temperature curve is a monotonically increasing smooth curve without an inflection point. The slope initially decreases and then increases, but remains always positive, indicating a supercritical phase;

(2) When (P = Pc), the temperature curve remains monotonically increasing, but the slope decreases to zero before increasing again, resulting in an inflection point. This curve represents the critical isobar, and the black hole is thermodynamically unstable at this point;

(3) When the pressure (P = 0.4Pc), the horizon radii are $r_h^1 = 0.1338$ and $r_h^2 = 0.7944$, respectively. This implies that when (P < Pc), within the range $r_h^1 < r_H < r_h^2$, the temperature curve exhibits non-monotonic behavior: initially increasing, then decreasing, and finally increasing again. When the pressure is below

the critical pressure, the black hole exhibits two-phase coexistence. This means that the black hole can exist in two distinct stable states: a smaller "liquid-like" state and a larger "gas- like" state, with an unstable intermediate state between them. This phase transition is analogous to the liquid-gas phase transition in van der Waals fluids.

Figure 3(b) and **3(c)** show the relationship between black hole temperature and shadow radius rs for non-commutative parameters α = 0.1 and α = 0.3, respectively. These representative values demonstrate that the shadow radius rs can replace the event horizon radius r_H to study the phase transition process of the non-commutative Schwarzschild-AdS black hole. When the pressure P is less than the critical pressure Pc: $r_s < r_s^1$ corresponds to a smaller stable black hole; $r_s^1 < r_s < r_s^2$ corresponds to a thermodynamically unstable black hole; and $r_s > r_s^2$ corresponds to a larger stable black hole. Furthermore, as the non-commutative parameter α increases, the region of thermodynamic instability expands, and both the shadow radius r_s and the temperature increase.

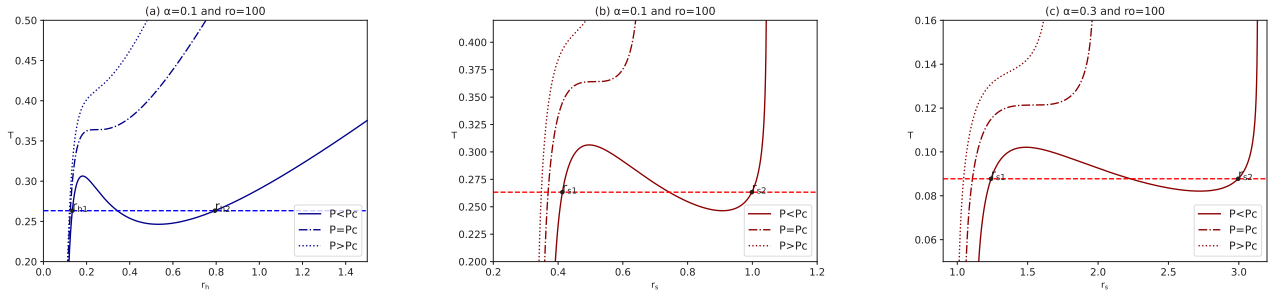

(a) (b) (c)

Figure 3. (a) Temperature as a function of r_H with α = 0.1, (b) temperature as a function of r_s with α = 0.1, (c) temperature as a function of r_s with α = 0.3. A static observer is located at r_0 = 100.

The order of a black hole's phase transition is closely associated with its heat capacity. In particular, a second-order phase transition at the thermodynamic critical point of a black hole can be characterized by a jump in heat capacity and a divergence in specific heat. Taking into account the relationship between entropy and area ($S = \frac{A}{4} = \pi r_H^2$) and the temperature from **Equation 28**, we can derive the heat capacity of a black hole under constant pressure.

$$C_P = T\left(\frac{\partial S}{\partial T}\right)_P = \frac{8\pi r_H^2(2r_H-\alpha)(3r_H+24P\pi r_H^3-3\alpha-16P\pi r_H^2\alpha)}{48P\pi r_H^4+12r_H\alpha-48P\pi r_H^3\alpha-3\alpha^2+2r_H^2(-3+8P\pi\alpha^2)} \quad (38)$$

The divergence of a black hole's heat capacity typically signifies system instability and suggests a possible phase transition. **Figure 4(a)** shows the relationship between the heat capacity of a non-commutative Schwarzschild AdS black hole and its event horizon radius under different pressures. **Figure 4(b)** and **4(c)** illustrate the relationship between heat capacity and shadow radius under the same conditions. The results show that the heat capacity diverges at the critical point, indicating a second-order phase transition in the black hole. The similar divergence of heat capacity at the critical point observed in **Figure 4(b)** and **4(c)** demonstrates that the shadow radius can be used to identify the order of the black hole phase transition.

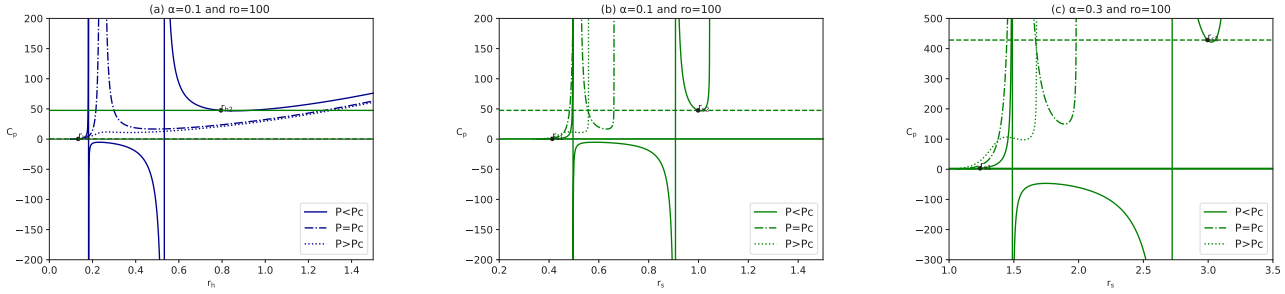

(a) (b) (c)

Figure 4. (a) The functional relationship between heat capacity and r_H when α = 0.1. (b) The functional relationship between heat capacity and r_s when α = 0.1. (c) The functional relationship between heat capacity and r_s when α = 0.3. A static observer is located at r_0 = 100.

5. Thermal profile of the Schwarzschild-AdS BH in non-commutative geometry

This section uses the thermodynamic profile of a black hole to intuitively reveal the relationship between the black hole shadow and its phase structure. The shadow contour curve in celestial coordinates can be expressed by the formula

$$x = \lim_{r\to\infty}\left(-r^2 sin\theta_0 \frac{d\Phi}{dr}\right)\Big|_{\theta_0\to\pi/2} \tag{39}$$

$$y = \lim_{r\to\infty}\left(r^2 \frac{d\theta}{dr}\right)\Big|_{\theta\to\pi/2} \tag{40}$$

For a static observer, **Figure 5** shows the shadow contour, where the shadow radius decreases with increasing pressure. **Figure 5(a)** and **5(b)** correspond to non-commutative parameters α = 0.1 and α = 0.3, respectively, showing that the shadow radius increases with increasing non-commutative parameter.

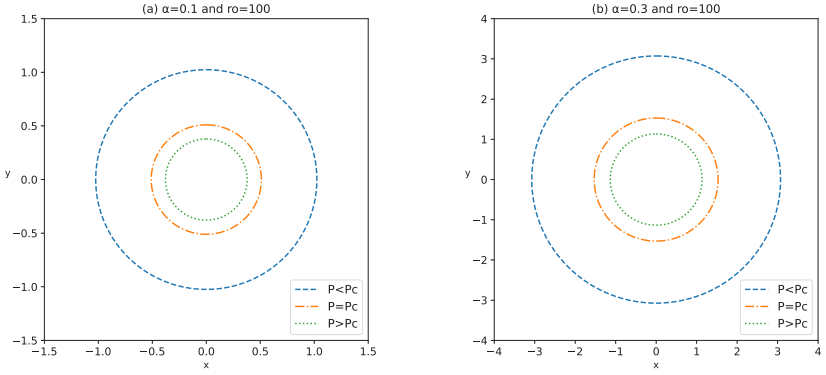

(a) (b)

Figure 5. Shadow profiles of a non-commutative Schwarzschild-AdS black hole. (a) Non-commutative parameter α = 0.1; (b) Non-commutative parameter α = 0.3. Here, the black hole mass M = 60, r_0 = 100.

Figure 6 presents the thermal distributions under three different pressures: P > Pc (supercritical phase), P = Pc (critical state), and P < Pc. The results are consistent with previous analyses: decreasing pressure leads to an

increased shadow radius, and increasing non-commutative parameter α also leads to an in increased shadow radius. **Figure 6(a)** and **6(b)** correspond to the supercritical phase (P > Pc), where the temperature gradually increases from the center, consistent with the dashed lines in **Figure 3**. **Figure 6(c)** and **6(d)** correspond to the critical state (P = Pc), which is thermodynamically unstable, and the temperature variation is also unstable, consistent with the dashed line segments in **Figure 3**. **Figure 6(e)** and **6(f)** correspond to the case P < Pc, where the temperature exhibits an ”N-type” variation: it initially increases, then decreases, and finally increases again, consistent with the solid lines in **Figure 3**.

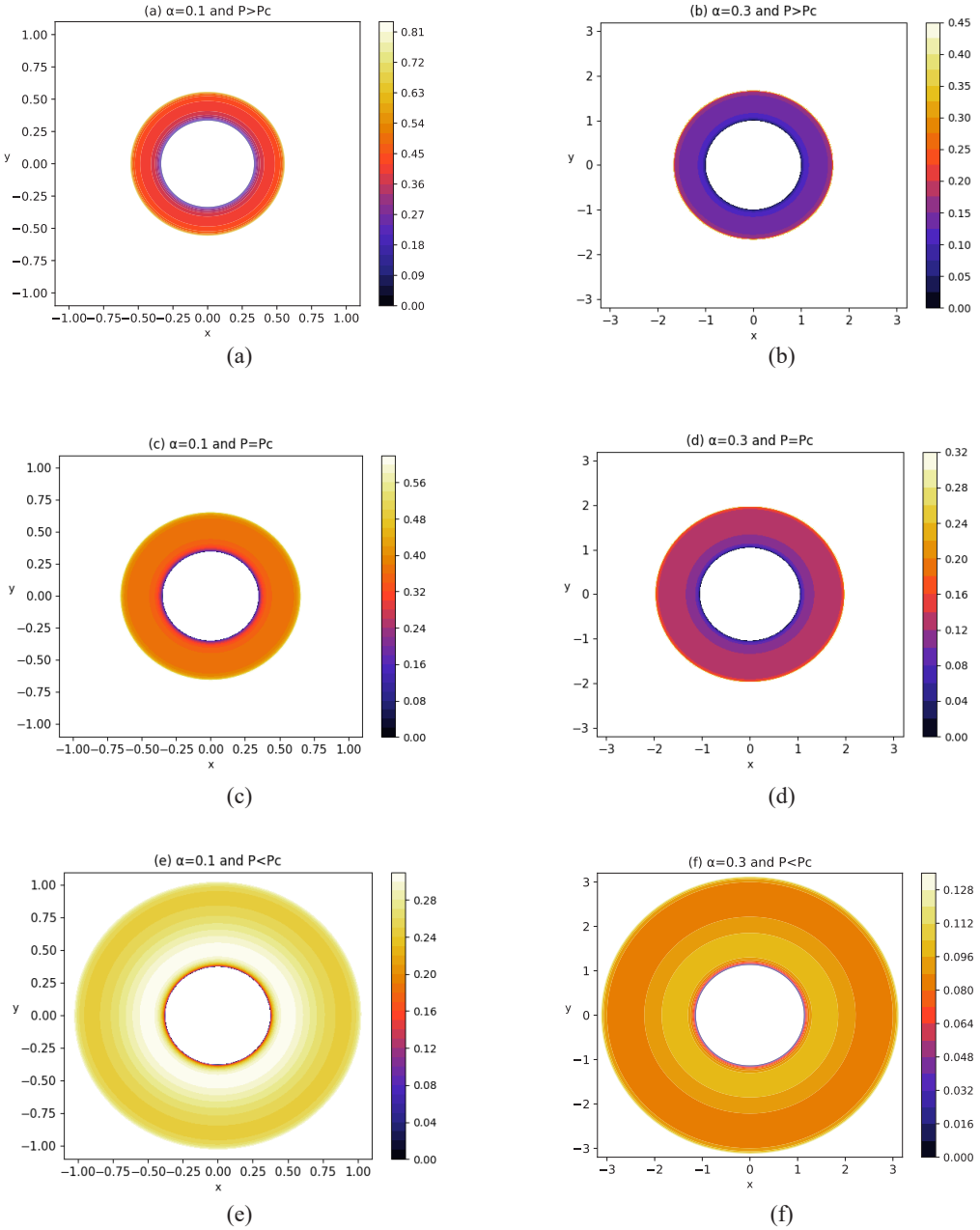

Figure 6. Thermodynamic profiles of non-commutative Schwarzschild-AdS black holes for diferent thermodynamic cases. (a) P > Pc,α = 0.1, (b) P > Pc,α = 0.3, (c) P = Pc,α = 0.1, (d) P = Pc,α = 0.3, (e) P < Pc,α = 0.1, (f) P < Pc,α = 0.1.

To more clearly show the ”N-type” temperature variation, **Figure 6** restricts the shadow radius range to r_s^1 to r_s^2, more prominently displaying the ”N-type” change. Therefore, the shadow radius can effectively replace the event horizon radius in describing the thermodynamic properties of the black hole. The obtained results are shown in **Figure 7**. Finally, the influence of the non-commutative parameter on the phase transition of the Schwarzschild-AdS black hole can also be clearly observed from **Figure 7**, and the obtained results are consistent with those in **Figure 3**.

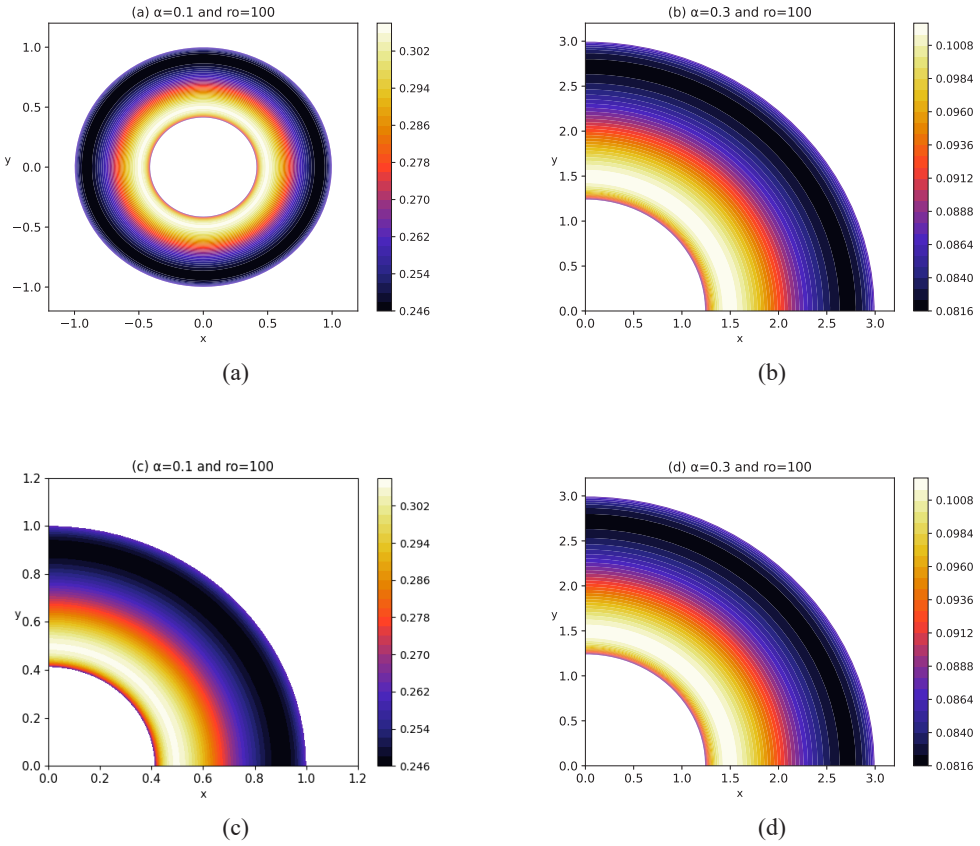

Figure 7. Thermodynamic profiles of non-commutative Schwarzschild-AdS black holes for diferent thermodynamic cases. (a) P < Pc,α = 0.1, (b) P < Pc,α = 0.3, (c) P < Pc,α = 0.1, (d) P < Pc,α = 0.3. (c) is a quarter of (a), (d) is a quarter of (b).

6. Conclusion

This paper investigates the phase transition of a Schwarzschild-AdS black hole within the framework of Non-Commutative Geometry by using the shadow radius as a substitute for the horizon radius. By utilizing the modified effective geometry incorporating the non- commutative parameter, a relationship between the shadow radius rs and the event horizon radius rh is established. The results indicate a positive correlation between them, implying that the black hole temperature can also be determined by the shadow radius. When r_0 =100 and the condition $f(r_0)$=1 is satisfied, **Equation (27)** can also be used to describe the relationship between the shadow radius and the event horizon for a Schwarzschild-AdS black hole. We present this relationship and observe that as the event horizon radius r_h increases, the shadow radius r_s also increases monotonically. Moreover, the growth trend of r_s gradually flattens out with further increase in r_h. Based on this, we argue that the shadow can be used to present

the phase transition structure of black hole thermodynamics. Based on the T–rh function, we further constructed the T–r_s function and meticulously analyzed the phase transition curves of the AdS black hole. When (P > Pc), the temperature curve is a monotonically increasing smooth curve without inflection points, indicating a supercritical phase. At the critical point (P = Pc), an inflection point appears on the temperature curve. This curve represents the critical isobar, and the black hole is thermodynamically unstable at this inflection point. When the pressure is below the critical pressure (P < Pc), the black hole exhibits two-phase coexistence, indicating that the black hole can exist in two distinct stable states. When the shadow radius is relatively small ($r_s < r_s1$), it corresponds to a smaller stable black hole; when the shadow radius falls within the range $r_s1 < r_s < r_s^2$, it corresponds to a thermodynamically unstable black hole; and when the shadow radius $r_s > r_s^2$, it corresponds to a larger stable black hole. The results indicate that the shadow radius r_s can be used as a substitute for the event horizon radius r_H to study the phase transition process of non-commutative Schwarzschild-AdS black holes. The results indicate that the shadow radius r_s can be used as a substitute for the event horizon radius r_h to study the phase transition process of a non-commutative Schwarzschild-AdS black hole. Subsequently, by combining the relationship between heat capacity and the event horizon radius, a relationship between heat capacity and the shadow radius is established to determine the order of the black hole phase transitions. In addition, the results also indicates that the heat capacity diverges at the critical point, implying the occurrence of a second-order phase transition in the black hole. This result is consistent with that obtained using the event horizon radius r_h. Finally, based on the T–r_s function, thermal profiles of the black hole were constructed for several representative sets of non-commutative parameters. It was found that the shadow radius is closely related to the pressure, exhibiting a decrease as the pressure increases. When (P < Pc), the temperature variation of the black hole exhibits an "increase → decrease → increase (N-shaped)" pattern. This indicates that the thermodynamics of the black hole can be fully captured by its thermal profile, and that the black hole shadow can indeed reflect the thermodynamic phase transition relations in the non-commutative Schwarzschild-AdS black hole. Furthermore, the influence of the non-commutative parameter on the thermodynamic phase transitions is thoroughly discussed throughout the article. Based on the above work, we conclude that the shadow can effectively serve as a substitute for the event horizon. This finding further advances further research into the thermodynamic phase transitions of black holes.

Funding

Sichuan Province Science and Education Joint Key Project (Project No.: 25LHJJ0097)

Disclosure statement

The authors declare no conflict of interest.

References

[1] Abbott B, Abbott R, Abbott T, et al. (LIGO Scientific and Virgo), 2017, GW170817: Observation of Gravitational Waves from a Binary Neutron Star Inspiral. Phys. Rev. Lett. 2017(119): 161101.

[2] Abbott B, Abbott R, Abbott T, et al. (LIGO Scientific and Virgo), 2019, Search for Gravitational Waves from Intermediate-Mass Black Hole Binaries in the Second and Third Observing Runs of LIGO and Virgo. Phys. Rev, 2019(X9): 031040.

[3] Gold R, et al. (Event Horizon Telescope), 2020, First M87 Event Horizon Telescope Results. V. Physical Origin of the Asymmetric Ring, ApJ 897, L23.
[4] Akiyama K, et al. (Event Horizon Telescope), 2022, First Sgr A Event Horizon Telescope Results. I. The Shadow of the Supermassive Black Hole in the Center of the Milky Way*, ApJ Lett. 930, L12 (2022).
[5] Akiyama K, et al. (Event Horizon Telescope), 2022, First Sgr A Event Horizon Telescope Results. II. EHT Array, Observations, and Data Processing*, ApJ Lett. 930, L13 (2022).
[6] Akiyama K, et al. (Event Horizon Telescope), 2022, First Sgr A Event Horizon Telescope Results. III. Imaging of the Galactic Center Supermassive Black Hole*, ApJ Lett. 930, L14 (2022).
[7] Akiyama K, et al. (Event Horizon Telescope), 2022, First Sgr A Event Horizon Telescope Results. IV. Variability, Morphology, and Black Hole Mass*, ApJ Lett. 930, L15 (2022).
[8] Akiyama K, et al. (Event Horizon Telescope), 2022, First Sgr A Event Horizon Telescope Results. V. Testing Astrophysical Models of the Galactic Center Black Hole*, ApJ Lett. 930, L16 (2022).
[9] Akiyama K, et al. (Event Horizon Telescope), 2022, First Sgr A Event Horizon Telescope Results. VI. The Shadow and Mass of the Central Black Hole*, ApJ Lett. 930, L17 (2022).
[10] Bardeen J, Press W, Teukolsky S, 1972, Rotating Black Holes: Locally Nonrotating Frames, Energy Extraction, and Scalar Synchrotron Radiation, ApJ 178, 347 (1972).
[11] Bozza V, 2010, Gravitational Lensing by Black Holes. Phys. Rev. D 82, 083005 (2010).
[12] Ma L, Lu H, 2020, Shadow of a Rotating Black Hole in Four-Dimensional Einstein-Gauss-Bonnet Gravity. Phys. Rev. D 102, 066018 (2020).
[13] Mishra A, Chakraborty S, Sarkar S, 2019, Black Hole Shadow in a Rotating Squashed Kaluza-Klein Black Hole Spacetime. Phys. Rev. D 100, 104054 (2019).
[14] Gralla S, Holz D, Wald R, 2019, Black Hole Shadows, Photon Rings, and Lensed Images. Phys. Rev. D 100, 024012 (2019).
[15] Jusufi K, Werner M, Banerjee A, et al., 2017, Shadow of a Rotating Five-Dimensional Black Hole in Braneworld. Phys. Rev. D 96, 024036 (2017).
[16] Jusufi K, Sarkar N, Rahaman F, et al., 2018, Shadow of a Charged Rotating Black Hole in Conformal Gravity. Phys. Rev. D 97, 104028 (2018).
[17] Pantig R, Yu P, Rodulfo E, et al., 2022, Shadow and Deflection Angle of Rotating Black Holes in Einstein-Maxwell-Weyl Gravity. Phys. Rev. D 105, 044034 (2022).
[18] Perlick V, Tsupko O, 2022, Gravitational Lensing by Black Holes: A Review. Phys. Rep. 963, 1 (2022).
[19] Synge J, 1966, The Escape of Photons from a Schwarzschild Field. Mon. Not. R. Astron. Soc. 131, 463 (1966).
[20] Luminet J, 1979, Image of a Spherical Black Hole with Thin Accretion Disk. Astron. Astrophys, 75, 229 (1979).
[21] Wang H, Wei S, 2022, Shadow of a Kerr-Newman Black Hole Surrounded by a Plasma. Phys. Rev. D 106, 024032 (2022).
[22] Wang H, Xu Y, Wei S, 2019, Shadow of a Rotating Black Hole in a Dark Matter Halo. Phys. Rev. D 100, 064052 (2019).
[23] Narayan R, Johnson M, Gammie C, 2019, Black Hole Shadows and Photon Rings: Observational Prospects. ApJ 884, L33 (2019).
[24] Guo S, Huang Y, Han Y, et al., 2023, Black Hole Shadow as a Probe of Dark Matter. ApJ 945, L23 (2023).
[25] Meng Y, Kuang X, Wang X, et al., 2023, Shadow of a Rotating Black Hole with a Cosmological Constant. Phys. Rev. D 107, 064059 (2023).

[26] Zeng W, Ling Y, Jiang Q, et al., 2023, Shadow of a Black Hole in f(R) Gravity. Phys. Rev. D 107, 084076 (2023).
[27] Zeng X, Zhang H, Zhang H, 2020, Shadow of a Rotating Black Hole in Einstein-Aether Theory. Phys. Rev. D 101, 044074 (2020).
[28] Zeng X, Zhang H, 2020, Shadow of a Black Hole in the Presence of a Global Monopole. Phys. Rev. D 102, 064033 (2020).
[29] He K, Guo S, Tan S, et al., 2022, Shadow of a Charged Black Hole with a Topological Defect. Phys. Rev. D 105, 104064 (2022).
[30] Peng J, Guo M, Feng X, 2021, Shadow of a Rotating Black Hole in Horndeski Gravity. Phys. Rev. D 104, 024058 (2021).
[31] Li G, He K, 2021, Shadow of a Black Hole in the Einstein-Maxwell-Scalar Theory. Phys. Rev. D 104, 024052 (2021).
[32] Zhou X, Chen S, Jing J, 2021, Shadow of a Rotating Black Hole in the Ghost-Free Bimetric Gravity. Phys. Rev. D 104, 024029 (2021).
[33] Zeng X, Yang C, Huang Y, et al., 2025, Black Hole Shadow and Thermodynamic Phase Transition. Phys. Rev. D 111, 044064 (2025).
[34] Li G, He K, 2021, Shadow of a Black Hole in the Einstein-Weyl Gravity. Phys. Rev. D 104, 044021 (2021).
[35] He K, Yang C, Zeng X, 2025, Correlation between Black Hole Shadow and Thermodynamic Criticality. Phys. Rev. D 111, 044078 (2025).
[36] Gan Q, Wang P, Wu H, et al., 2021, Shadow of a Rotating Black Hole in the Einstein-Born-Infeld Gravity. Phys. Rev. D 104, 044073 (2021).
[37] Guo S, He K, Li G, et al., 2021, Shadow of a Black Hole in the Einstein-Maxwell-Dilation Theory. Phys. Rev. D 104, 044024 (2021).
[38] Zeng X, He K, Li G, et al., 2022, Black Hole Shadow in the Presence of a Magnetic Field. Eur. Phys. J. C 82, 764 (2022).
[39] Hawking S, 1976, Particle Creation by Black Holes. Commun. Math. Phys. 43, 199 (1975), [Erratum: Commun. Math. Phys. 46, 206 (1976)].
[40] Bekenstein J, 1994, Black Holes: Classical Properties, Thermodynamics, and Heuristic Quantization. Phys. Rev. D 49, 1912 (1994).
[41] Kubiznak D, Mann R, 2012, P-V Criticality of Charged AdS Black Holes. JHEP 07, 033 (2012).
[42] Cai R, Cao L,Li L, et al., 2013, P-V Criticality in the Extended Phase Space of Gauss-Bonnet Black Holes in AdS Space. JHEP 09, 005 (2013).
[43] He K, He X, Hu X, et al., 2019, Thermodynamic Geometry and Critical Phenomena of AdS Black Holes with Nonlinear Electrodynamics. Chin. Phys. C 43, 125101 (2019).
[44] Ökcü B, Aydiner E, 2024, Joule-Thomson Expansion of AdS Black Holes. Eur. Phys. J. C 77, 24 (2024).
[45] Wei S, Liu Y, 2018, Thermodynamic Phase Transition of Kerr-AdS Black Holes. Phys. Rev. D 97, 104027 (2018).
[46] Zhang M, Guo M, 2020, Thermodynamic Geometry of AdS Black Holes in f(R) Gravity. Eur. Phys. J. C 80, 790 (2020).
[47] Belhaj A, Chakhchi L, Moumni H, et al., 2020, Thermodynamic Criticality of AdS Black Holes in Higher Dimensions. Int. J. Mod. Phys. A 35, 2050170 (2020).
[48] Guo S, Li G, Liang E, 2022, Thermodynamic Phase Transition of Black Holes with a Cosmological Constant. Phys. Rev. D 105, 023024 (2022).
[49] Nicolini P, 2009, Noncommutative Black Holes: A Review. Int. J. Mod. Phys. A 24, 1229 (2009).

[50] Snyder H, 1947, Quantized Space-Time. Phys. Rev. 71, 38 (1947).
[51] Li G, He J, Chen B, 2021, Noncommutative Black Hole Thermodynamics. Chin. Phys. C 45, 015111 (2021).
[52] Aschieri P, Blohmann C, Dimitrijevic M, et al., 2005, A Gravity Theory on Noncommutative Spaces. Class. Quant. Grav. 22, 3511 (2005).
[53] Aschieri P, Dimitrijevic M, Meyer F, et al., 2006, Noncommutative Geometry and Gravity. Class. Quant. Grav. 23, 1883 (2006).
[54] Zeng X, Zeng G, Li G, et al., 2022,, Noncommutative Corrections to Black Hole Shadow. Nucl. Phys. B 974, 115639 (2022).
[55] Zeng X, Aslam M, Saleem R, 2023, Noncommutative Black Hole Shadow and Thermodynamic Phase Transition. Eur. Phys. J. C 83, 129 (2023).
[56] Nicolini P, Smailagic A, Spallucci E, 2005, Noncommutative Geometry Inspired Schwarzschild Black Hole. Phys. Lett. B 632, 547 (2005).
[57] Nozari K, Mehdipour S, 2008, Noncommutative Inspired Black Holes in Extra Dimensions. Class. Quant. Grav. 25, 175015 (2008).
[58] Wang R, Ma S, You L, et al., 2025,, Noncommutative Corrections to Kerr Black Hole Shadow. Chin. Phys. C 49, 065101 (2025).
[59] Anacleto M, Brito F, Campos J, et al., 2023, Noncommutative Black Hole Thermodynamics and Phase Transition. Eur. Phys. J. C 83, 298 (2023).
[60] Zheng H, Mou P, Chen Y, et al., 2023, Black Hole Shadow in Noncommutative Geometry. Chin. Phys. B 32, 080401 (2023).